



Voltage and frequency dependence of prestin-associated charge transfer

Sean X. Sun^{a,c}, Brenda Farrell^b, Matthew S. Chana^c, George Oster^d,
William E. Brownell^b, Alexander A. Spector^{a,c,*}

^a Department of Mechanical Engineering, Johns Hopkins University, Baltimore, MD, USA

^b Bobby R. Alford Department of Otolaryngology Head and Neck Surgery, Baylor College of Medicine, Houston, TX, USA

^c Department of Biomedical Engineering, Johns Hopkins University, 720 Rutland Ave., Traylor 411, Baltimore, MD, USA

^d Department of Molecular and Cellular Biology, University of California Berkeley, Berkeley, CA, USA

ARTICLE INFO

Article history:

Received 23 October 2008

Received in revised form

7 May 2009

Accepted 12 May 2009

Available online 31 May 2009

Keywords:

Electro-diffusion model

Membrane motor complex

Non-linear capacitance

High frequency

ABSTRACT

Membrane protein prestin is a critical component of the motor complex that generates forces and dimensional changes in cells in response to changes in the cell membrane potential. In its native cochlear outer hair cell, prestin is crucial to the amplification and frequency selectivity of the mammalian ear up to frequencies of tens of kHz. Other cells transfected with prestin acquire voltage-dependent properties similar to those of the native cell. The protein performance is critically dependent on chloride ions, and intrinsic protein charges also play a role. We propose an electro-diffusion model to reveal the frequency and voltage dependence of electric charge transfer by prestin. The movement of the combined charge (i.e., anion and protein charges) across the membrane is described with a Fokker–Planck equation coupled to a kinetic equation that describes the binding of chloride ions to prestin. We found a voltage- and frequency-dependent phase shift between the transferred charge and the applied electric field that determines capacitive and resistive components of the transferred charge. The phase shift monotonically decreases from zero to -90° as a function of frequency. The capacitive component as a function of voltage is bell-shaped, and decreases with frequency. The resistive component is bell-shaped for both voltage and frequency. The capacitive and resistive components are similar to experimental measurements of charge transfer at high frequencies. The revealed nature of the transferred charge can help reconcile the high-frequency electrical and mechanical observations associated with prestin, and it is important for further analysis of the structure and function of this protein.

© 2009 Elsevier Ltd. All rights reserved.

1. Introduction

Outer hair cells found in the cochlea of the mammalian ear have a unique form of motility, called electromotility, resulting from changes in the transmembrane electric field (Brownell et al., 1985; Ashmore, 1987; Santos-Sacchi and Dilger, 1988). The major features of electromotility are the cell dimensional changes, active force production, and transfer of charge across the membrane observed within a broad range of acoustic frequencies (Brownell et al., 2001; Spector et al., 2006, for review). Prestin, a membrane protein expressed in the plasma membrane of outer hair cells, is required for the outer hair cell to exhibit electromotility (Lieberman et al., 2002; Dallos et al., 2008). This membrane protein is a member of a solute carrier/anion transporter family (Zheng et al., 2000; Schlaechenger and Oliver, 2007). Hydrophobic analysis

suggests there are up to 12 transmembrane domains in prestin (Zheng et al., 2001). Evolutionary trace analysis of the protein reveals an important role of residues near the conserved sulfate transporter domain (Rajagopalan et al., 2006). The secondary and tertiary structures of this protein are unknown (Dallos and Fakler, 2002; Deak et al., 2005; Navaratnam et al., 2005; He et al., 2006, for review).

Non-motile cells transfected with prestin acquire electromotile features, including dimensional changes, force production, and charge transfer that is readily measured by electrophysiological techniques (Zheng et al., 2000; Rajagopalan et al., 2006). Experimental measurements show that the total charge moved in response to change in transmembrane electric field exhibits a sigmoidal charge–voltage function for both outer hair cells and prestin-transfected cells where the derivative of the charge with respect to the voltage exhibits a characteristic bell-shaped capacitance–voltage function. Prestin-associated charge movement requires intracellular chloride ions (Oliver et al., 2001). Intrinsic protein charges also play a role. When charged residues are replaced by non-charged residues the magnitude of charge

* Corresponding author at: Department of Biomedical Engineering, Johns Hopkins University, 720 Rutland Ave., Traylor 411, Baltimore, MD, USA. Tel.: +1 410 502 6955.

E-mail address: aspector@jhu.edu (A.A. Spector).

transferred does not change, but there is a translation of its voltage dependence along the voltage axis (Oliver et al., 2001). The exact composition of the transferred charge and mechanism by which it is transferred by prestin are not experimentally established; several models are proposed (Oliver et al., 2001; Rybalchenko and Santos-Sacchi, 2003; Muallem and Ashmore, 2006) to explain the dependence of charge movement on ion concentration and other parameters.

A displacement current (charge transfer across the membrane as opposed to through the membrane) is measured for a variety of biomembrane-based processes. In addition to prestin-associated charge movement, it is also observed when hydrophobic anions are dissolved in membranes (e.g., Benz and Nonner, 1981; Lu et al., 1995); when voltage-gated ion channels are stimulated (e.g., Fernandez et al., 1983); and for ion movement by transporters (Lu et al., 1995). In all cases a sigmoidal displacement charge–voltage function and a corresponding bell-shaped capacitance–voltage function is observed. The displacement charge is often described with a two-state Boltzmann function (e.g., Huang and Santos-Sacchi, 1994; Gale and Ashmore, 1997b). Although this discrete model describes the experimental data obtained from outer hair cells and prestin-expressing cells it does not provide a unique solution; it is not possible to determine the number of charged states within the membrane by fitting the experimental data to a two or multiple-state Boltzmann function (Scherer and Gummer, 2004).

We introduce an alternative approach and propose an electro-diffusion model of prestin-associated charge transfer. The model includes binding chloride ions to the protein with the subsequent diffusion of charge across the membrane. We interpret this charge as a combination of bound chloride ions together with internal protein charges. The dynamics of charge translocation in an electric field is described by the high friction limit of the Fokker–Planck (or Smoluchowski) equation. While the Fokker–Planck approach has been used for a variety of biophysical problems this is the first time it has been incorporated into a model of prestin-associated charge transfer. At steady state under a DC electric field the problem has an analytical solution of sigmoidal shape. Under an AC field the solution reveals a voltage- and frequency-dependent phase shift (delay) between the applied electric field and the transferred charge which results in capacitive and resistive components of the charge. The total amount of charge and its capacitive component both monotonically decrease with frequency, while the resistive component has a maximum as a function of frequency. These results are consistent with experimental observations (Lu et al., 1995; Farrell et al., 2006). By comparing measurements of charge transfer obtained at frequencies up to several tens of kilohertz (Gale and Ashmore, 1997a,b) with our model we estimate the diffusion coefficient for charge transfer in prestin. This insight into the frequency-dependence of the charge movement is important (Gale and Ashmore, 1997a,b; Frank et al., 1999; Ludwig et al., 2001; Liao et al., 2007) because outer hair cells and presumably prestin provide the active component of hearing at acoustic frequencies.

The proposed modeling framework is also a general approach for understanding voltage- and frequency-dependent properties of ion motive membrane proteins. By considering an energy landscape picture within the Fokker–Planck equation, a microscopic picture of the charge transfer process is analyzed. This approach is also well suited for understanding additional influences such as lipid composition and membrane tension on the charge transfer process. Phenomenological kinetic constants can also describe the charge transfer process. However, the relationship between the kinetic constants and external influences are not clear. Using the Fokker–Planck equation framework,

we not only obtain an estimate of the physical diffusion constant of prestin movement, we also derive the phase shift between the applied field and transferred charge along with the capacitive and resistive components of the charge and present these three characteristics as function of voltage and frequency. The latter result is also a generic property of voltage-dependent ion transporters (Lu et al., 1995).

2. A model of electric charge transfer by prestin

2.1. Conceptual description

A conceptual sketch of the prestin system is shown in Fig. 1. The interaction of the protein with the intracellular chloride is described in terms of the probabilities of binding and detachment P and $1-P$, respectively, and the corresponding rate constants, k_1 and k_{-1} . The total charge movement per molecule probably involves anions and protein charges, and we assume that a collective movement of the protein and chloride results in a net translocation of a charge (Fig. 1a). The charge movement across the membrane (z -direction) is described by a function $\rho(z,t)$ defined as the probability density of observing the average position of the charge system at point z and time t (Fig. 1b). While prestin-associated charge may follow a 3-D trajectory, we consider movement in the z -direction reported in experiments. To define the “transferred” charge, we separate total width of the protein, L , into two parts with lengths $(1-l^*)L$ and l^*L , respectively, where l^* is a non-dimensional number such that $0 \leq l^* \leq 1$. The charge is considered “transferred” if it reaches the part l^*L part of the protein (Fig. 1b). In this model, we assume that the charge is not transported out of the membrane (currently, there is no experimental evidence that prestin is a full transporter), however this condition can be relaxed if new experimental information on charge transport through the membrane becomes available (see also Results and Discussion).

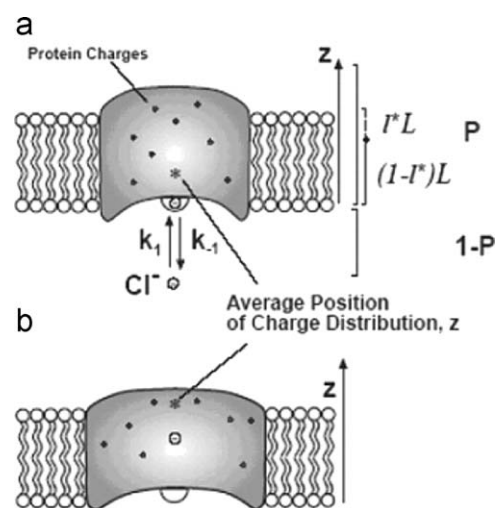


Fig. 1. Conceptual description of our model of electric charge transfer by prestin: (a) chloride ions (minus sphere) are in the cytoplasm and can bind to the protein with association and disassociation rates k_1 and k_{-1} . The probabilities of the ion being inside and outside of the protein are P and $1-P$, respectively. We consider the combined charge of the ion and internal charges of the protein (dark circles). The translocation of the combined charge is characterized by changes in the average position of charge distribution (asterisk) along the z -direction. In our model, this position is described by the probability density, $\rho(z,t)$. Two regions of the membrane, defined by l^* and $(1-l^*)$ relative lengths are shown, indicating the upper and lower parts of the membrane; (b) the combined charge has moved to the upper part of the membrane. The movement was driven by the transmembrane electric field and results in conformational changes in the protein.

When an AC electric field is applied across the membrane there is a phase shift between the transferred charge and the applied field. We introduce a capacitive (in phase with the applied field) and resistive (90°-phase delay) component of the transferred charge. The time derivative of the capacitive component represents the displacement current, which is associated with the non-linear capacitance reported in experiments (e.g., Huang and Santos-Sacchi, 1994; Gale and Ashmore, 1997b). The time derivative of the resistive component is in phase with the field, like an ohmic current also measured in experiments (Lu et al., 1995; Farrell et al., 2006).

To analyze the dynamics of charge movement and chloride binding, we introduce a set of coupled equations. A Fokker–Planck equation is used to compute the time-dependent behavior of $\rho(z,t)$, a kinetic equation is used to model ion binding which supplies a boundary condition for the Fokker–Planck equation. The proposed approach is physical and contains the effect of the applied field explicitly. A limitation occurs when the frequency of the applied field becomes very large (>MHz). In this limit, the relaxation time scale of the surrounding polarizable medium comes into play and the Markovian approximation breaks down. We start by assuming that prestin works up to the kHz regime where the Markovian-type models are valid.

2.2. Mathematical formulation

The binding kinetics is described by the equation

$$\frac{dP}{dt} = k_1(1 - P) - k_{-1}P \quad (1)$$

where k_1 is proportional to the concentration of intracellular chloride. The movement of the charge in the z -direction is described by the Fokker–Planck equation

$$\frac{\partial \rho}{\partial t} = -\frac{\partial J}{\partial z} = \frac{\partial}{\partial z} \left(\frac{D}{kT} \frac{\partial V}{\partial z} \rho + D \frac{\partial \rho}{\partial z} \right) \quad (2)$$

where J is the probability flux, V is the free energy of the prestin system as a function of the vertical distance, z , that determines the drift term in the flux, D is the diffusion coefficient, k is the Boltzmann constant, T is the absolute temperature, and the ratio kT/D can be considered as the effective coefficient of drag (Xing et al., 2005).

The free energy of the system as a function of the charge position contains several contributions: (1) electrostatic energy of the moving charge distribution, (2) conformational energy of the protein, and (3) response of the membrane to the protein conformational change, including the effects of various membrane components (i.e., cholesterol). In the current model, we consider the electrostatic component of the free energy only. In this component of the free energy, we take into account the externally applied electric field and introduce an additional term to reflect the effect of the charge distribution inside the protein. We present the electrostatic energy gradient as $-\partial V/\partial z = q\Psi/L$ where q is the magnitude of the moving charge, and Ψ is the electric potential. We decompose potential Ψ into DC and AC components

$$\Psi = \Psi_{DC} + \Psi_{AC} \quad (3)$$

where

$$\Psi_{DC} = \Psi_{DC}^i + \Psi_{DC}^e \quad (4)$$

and

$$\Psi_{AC} = \Psi_{AC}^e \sin \omega t \quad (5)$$

Here ω is the frequency of the AC stimulus and the superscripts i and e correspond to the internal protein and external applied electric fields, respectively, and Ψ_{DC}^i is the potential reflecting the

protein charges. For the purpose of comparing our model with experimental recordings of prestin-associated charge movement we assume that Ψ is equivalent to the measured membrane potential.

By substituting the electrostatic energy term into Eq. (2) the Fokker–Planck equation becomes

$$\frac{\partial \rho}{\partial t} = D \left(-\frac{q\Psi}{kTL} \frac{\partial \rho}{\partial z} + \frac{\partial^2 \rho}{\partial z^2} \right) \quad (6)$$

and is solved with boundary conditions

$$J(t, z = 0) = \frac{dP}{dt} \quad \text{and} \quad J(t, z = L) = 0 \quad (7)$$

where the first condition is governed by the kinetics of chloride binding (see Eq. (1)) and the second stipulates that there is no transport out of or into the membrane at $z = L$, although the boundary condition at $z = L$ can be relaxed to include different assumptions on charge transport by prestin. After we determine $\rho(z,t)$, the total probability of charge transfer is calculated as

$$P^* = \int_{L(1-\Gamma)}^L \rho(t, z) dz \quad (8)$$

In the case of application of AC electric fields, the amplitude of probability P^* is used to introduce capacitive, $P_c = P^* \cos \theta$, and resistive, $P_r = -P^* \sin \theta$, components of the transferred charge, where θ is the negative phase shift between the charge and the AC applied field.

2.3. Method of the solution and parameter estimation

Eq. (6) was solved numerically by using FemLab (Comsol) software. The steady state solution ($\partial \rho/\partial t = 0$) of Eq. (6) under the application of a DC electric field can be found analytically. This solution takes the following form:

$$\rho(z) = \frac{\beta e^{\beta z}}{(e^{\beta L} - 1)^\gamma} \quad (9)$$

where

$$\beta = q\Psi/kTL \quad \text{and} \quad \gamma = 1 + k_{-1}/k_1$$

The total probability that the charge is transferred, P^* , is then given by the equation

$$P^* = \frac{1 - e^{-\beta L}}{(1 - e^{-\beta L})^\gamma} \quad (10)$$

We used the analytical solution (Eqs. (9) and (10)) to test the accuracy of the computational results. In the computational steady state solution, we integrate the Fokker–Planck equation until stabilization of the probability density $\rho(t, z)$ at any z inside the protein.

Our model includes three main parameters, the dimensionless length, l^* , charge, q , and an effective diffusion coefficient, D , that determine prestin-associated charge transfer under the action of DC or (and) AC electric field. To estimate parameters l^* and q , we consider the case when the system subjected to a DC field reaches its steady state. The experimental charge–voltage function is typically fit with a two-state Boltzmann function (Gale and Ashmore, 1994, 1997b; Huang and Santos-Sacchi, 1994; Oliver et al., 2001)

$$Q/Q_{\max} = \frac{1}{1 + \exp[-(\Psi - \Psi^*)/\alpha]} \quad (11)$$

with Q_{\max} , α , and Ψ^* as parameters. In the case of DC fields, the transferred charge Q is represented by the function $P^*(\Psi_{DC}^e)$. While the first approximations of parameters l^* and q can be extracted from the data in Fig. 2a and b where the normalized computed

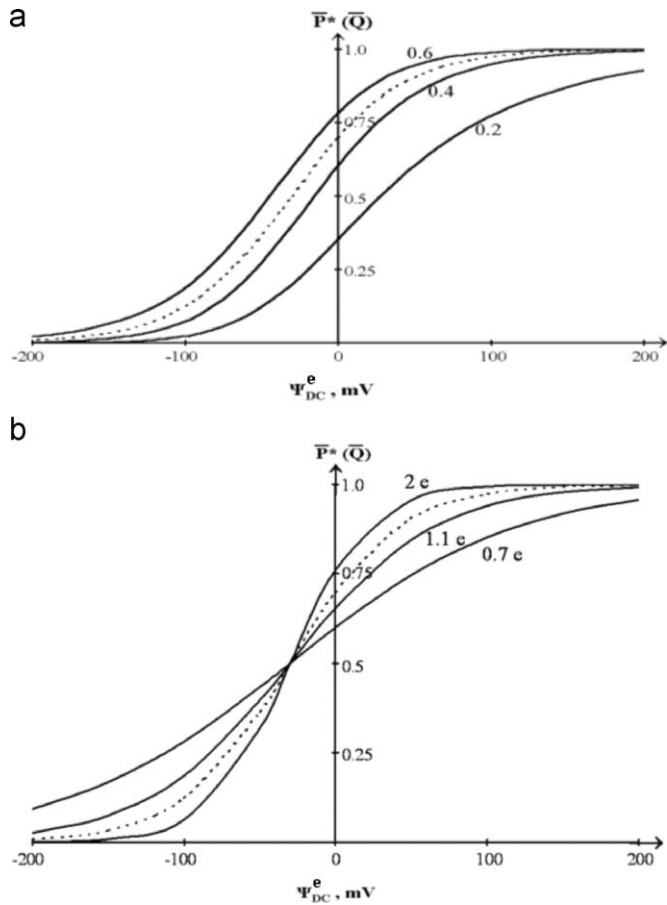


Fig. 2. Normalized probability of the charge transfer, P^* , as a function of the applied DC component of the membrane potential, Ψ_{DC}^e , (solid lines) vs. normalized experimental charge transferred by prestin in the outer hair cell membrane, \bar{Q} (dashed lines); $\Psi_{DC}^e = 30$ mV: (a) effect of relative length l^* ($l^* = 0.2$; 0.4; and 0.6), on P^* and (b) effect of charge q on P^* ($q = 0.7e$; 1.1e; and 2e).

probability $\bar{P}^*(\Psi_{DC}^e)$ is plotted for different values of l^* and q vs. normalized experimental charge, \bar{Q} , we make accurate estimates of the two parameters by minimizing an error function. The error function is defined as

$$Er(l^*, q) = \sum_i [P^*(l^*, q, \Psi_i) - \bar{Q}(\Psi_i)]^2 \quad (12)$$

where Ψ_i are points along the voltage axis and the normalized experimental charge, \bar{Q} , is described by Eq. (11) with parameters $\alpha = 33$ mV and $\Psi^* = -30$ mV that are close (supplemental Table 1) to those in (Gale and Ashmore, 1994, 1997b; Huang and Santos-Sacchi, 1994). As a result of the minimization of the error function (supplemental Fig. 1), we obtain $l^* = 0.5$ and $q = 1.5e$ (average charge per molecule). Parameter α in Eq. (11) is equal to $(kT/\delta ne)$, where δ is fraction of the membrane thickness traversed by the charge, and n is valence. The product of our model parameters q and $1-l^*$ is similar to the product of the denominator in the above expression for α . Our estimates result in $q(1-l^*) = 0.75$ which is close to previous estimates of δne .

To estimate the diffusion coefficient, we use experimental measurements of the capacitance–voltage functions under high-frequency conditions (Gale and Ashmore, 1997a). In our modeling, we consider the harmonic regime of the charge movement generated by the application of an external AC electric field. The probability P^* will depend on the ratio k_{-1}/k_1 , however, the relative decrease in P^* with frequency is independent of that ratio. We use the values of the parameters l^* and q estimated from the

previous analysis of the steady state, and determine D from the relative decrease of the calculated P^* with increasing frequency. We do this by comparing the measured decrease in nonlinear capacitance (Gale and Ashmore, 1997a) with our calculations. Assuming the protein spans the thickness of membrane at ~ 4.5 nm, we estimate $D = 0.5 \times 10^{-8}$ cm²/s. More discussion of the diffusion coefficient is presented in the next section.

3. Results and discussion

3.1. P^* -probability as a measure of transferred charge

We analyze the effects of l^* and q parameters and compare our model results to experimental data obtained from outer hair cells at low frequencies (< 1 kHz) with whole cell recordings of charge transfer. Fig. 2a shows the normalized probability of the transferred charge, \bar{P}^* , as a function of the DC membrane potential for three different l^* values, 0.2, 0.4, and 0.6. Fig. 2b presents this probability vs. the DC membrane potential for different q -values, 0.7e, 1.1e, and 2e. In Fig. 2a and b, the solid lines correspond to the computed charge, \bar{P}^* , where the dashed lines represent experimentally determined Q – Ψ functions observed in outer hair cells.

Our model describes prestin-associated charge transfer as observed in outer hair cells (Gale and Ashmore, 1994, 1997b; Huang and Santos-Sacchi, 1994; Oliver et al., 2001) and prestin-expressing mammalian cultured cells (Zheng et al., 2000; Rajagopalan et al., 2006). The magnitude of l^* (which reflects the portion of the protein traversed by the charge) translates the P^* – Ψ function along the voltage axis, an increase/decrease results in a shift in the hyperpolarization/depolarization directions (Fig. 2a). Likewise an increase (decrease) in the magnitude of charge q results in a steeper (shallower) P^* – Ψ function (Fig. 2b). In the steady state case, when the time derivative is equal to zero, Eq. (2) reduces to a 1st-order ODE and it can be solved analytically (Eqs. (9) and (10)). By comparing our model results with experimental data, we find an l^* of 0.5 and q of 1.5e where product of q and $1-l^*$ is equal to 0.75, and is consistent with previous two-state Boltzmann-function estimates (Gale and Ashmore, 1994, 1997b; Iwasa, 1994; Santos-Sacchi et al., 1998).

3.2. Capacitive part of the transferred charge and estimation of the effective diffusion coefficient

We compare our model to experimental data obtained from outer hair cells at high frequencies with cell-attached recordings of charge transfer to determine D . In Figs. 3 and 4, an AC electric field of a constant amplitude and variable frequency is applied

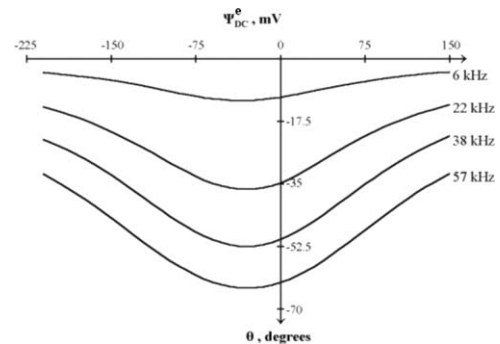


Fig. 3. Frequency effects on charge transfer by prestin. The phase shift between the transferred charge and the applied AC component of the membrane potential vs. the applied DC component of the membrane potential for four different frequencies.

with a DC membrane potential. Fig. 3 presents the phase shift between the probability of charge being transferred relative to the AC potential applied for frequencies from 6 through 57 kHz. Fig. 4a shows the amplitudes of that probability for the same frequencies. The amplitudes are normalized by the maximum low-frequency P^* (reached at $\Psi_{DC}^e = -30\text{ mV}$ ($\Psi_{DC}^i = 30\text{ mV}$) for $l^* = 0.5$ and $q = 1.5e$). In Fig. 4b and c, we present the capacitive and resistive components of the transferred charge. Also, Fig. 4d shows the computed resistive component of the charge along with experimental data (Lu et al., 1995). Finally, Fig. 4e shows the absolute value of phase shift and the ratio of the resistive to capacitive component (left and right vertical axes, respectively) as functions of frequency.

To analyze both the voltage and frequency effects of prestin-associated charge movement, we perturbed our model with an AC field riding on a DC field. In this case, the capacitive component of the charge was defined as the product of the total charge amplitude and the cosine of the phase shift between the charge and the electric field. At any given frequency, the capacitive component was bell-shaped as a function of voltage (Fig. 4b), and it reached its maximum at $\Psi_{DC}^e = -30\text{ mV}$. Our high-frequency solution is mainly determined by the coefficient of diffusion across the membrane of the combined charge. Parameters l^* and q play a role too, but in our frequency analysis (Figs. 3 and 4), we keep them at their optimal values. Experimental data in (Gale and Ashmore, 1997a) present outer hair cell nonlinear capacitance as a function of frequency. We compare our model with this data and calculate a value of D ($0.5 \times 10^{-8}\text{ cm}^2/\text{s}$) that causes a 50% decrease in P_c ($P^* \cos \theta$) at 30 kHz. The estimated diffusion coefficient is smaller than for the diffusivity of chloride ions in solution (about $10^{-5}\text{ cm}^2/\text{s}$ (Hille, 1984)) and greater than the diffusivity for membrane proteins (about 10^{-11} – $10^{-10}\text{ cm}^2/\text{s}$, (Axelrod et al., 1976; Jechiel and Edidin, 1987)). Also, our diffusion coefficient is close to that for the diffusivity of lipids (Oghalai et al., 2000; de Monvel et al., 2006) in outer hair cell membranes. This is consistent with our interpretation of the diffusion coefficient as an effective parameter reflecting interactions among main components of the prestin system, including chloride ions, protein, and membrane environment. While the primary mode of the charge movement is most likely in z-direction (normally to the membrane), it is coupled with in-plane movement of the prestin system, which influences the value of D .

We developed an additional test to confirm our estimate of the diffusion coefficient on the basis of the experiments of Gale and Ashmore (1997a). We consider the transient regime of the charge transfer upon application of a voltage step. In our model, the transient component of the transferred charge is represented by

dP^*/dt , and the kinetics of the corresponding process is fully determined by the diffusion coefficient. Thus, we also estimated the diffusion coefficient by minimizing the difference between the experimental transient currents (Gale and Ashmore, 1997a) and

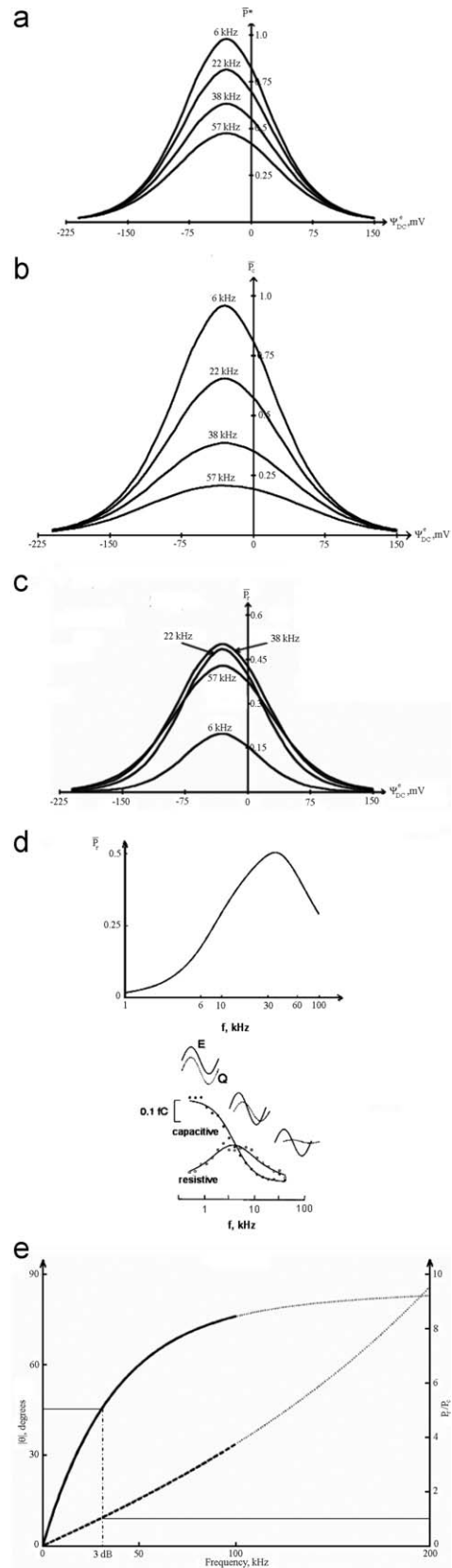


Fig. 4. Frequency effects on charge transfer by prestin ($l^* = 0.5$, $q = 1.5$). Characteristics of the transferred charge in response to the application of AC electric fields as functions of the DC component of the membrane potential for four different frequencies. Frequency dependence of the charge components and its comparison with experimental data: (a) normalized amplitude of the transferred charge, (b) normalized capacitive component of the transferred charge, (c) normalized resistive component of the transferred charge, (d) upper panel: normalized resistive component of the transferred charge as a function of frequency at $\Psi_{DC}^e = -30\text{ mV}$; lower panel: experimental data for different components of charge transfer associated with a hydrophobic ion dipicrylamine (DPA) movement across the membrane within a broad frequency range (modified from Lu et al., 1995); three sinusoidal curves show the measured charge, Q , vs. applied electric field, E , also the charge amplitude decreases and Q - E phase shift increases with frequency; the capacitive component of the charge monotonically decreases with frequency; and the resistive component of the charge is bell-shaped and has a single maximum like the theoretical curve in the upper panel, and (e) absolute value of the phase shift (solid line and left axis) and ratio of the resistive to capacitive components of the transferred charge (short-dashed line and right axis); dotted lines are used for both characteristics beyond 100 kHz to show the asymptotic behavior of the computed characteristics. The long-dashed lines show the 3 dB frequency that corresponds to 45° and ratio of P_r/P_c equal to 1.

our model results. This additional estimate resulted in a similar value: the difference between two coefficients was within 1.5–2 times depending on the DC resting and increment potentials.

We also consider the frequency dependence of the transferred charge for different diffusion coefficients. Fig. 5 presents the total charge (a) and its capacitive component (b) vs. frequency for three different diffusion coefficients, 0.5, 0.8, and 1.1×10^{-8} where the first of them is the above estimate and two other are larger but on the same order of magnitude. Two particular frequencies corresponding to 50%- and 3 dB ($1/\sqrt{2}$)-decrease are shown in Fig. 5. In general, the higher the diffusion coefficient, the better is the frequency response of the protein and the greater are both 3-dB and 50%, frequencies. Table 1 summarizes the values of these two frequencies for the total charge and capacitive component estimated at each of three diffusion coefficients under consideration.

There is a discrepancy in 3-dB and 50%, frequencies for the charge transfer (Gale and Ashmore, 1997a) and electromotility/force production (Frank et al., 1999) of OHCs. It is possible to reconcile the difference if both capacitive and resistive

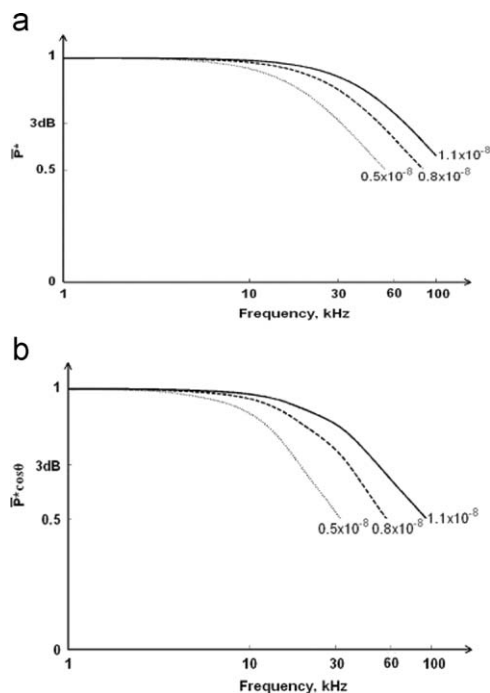


Fig. 5. Frequency-dependence of the total transferred charge: (a) and its capacitive component; (b) for three different diffusion coefficients, 0.5 (dotted lines), 0.8 (dashed lines), and 1.1×10^{-8} cm²/s (solid lines). Here total charge and its capacitive component are represented by maximal values ($\Psi_{DC}^e = -30$ mV) of the P^* and P_c amplitudes. Two important values corresponding to 3 dB- and 50%-decrease are marked on the vertical axes.

Table 1
3-dB- and 50%-decrease frequencies (kHz) for the total transferred charge and its capacitive component for three diffusion coefficients, 0.5, 0.8, and 1.1×10^{-8} cm²/s.

D (cm ² /s)	0.5×10^{-8}	0.8×10^{-8}	1.1×10^{-8}
$f_{3\text{ dB}}(P^*)$, kHz	31	50	69
$f_{50\%}(P^*)$, kHz	54	86	108
$f_{3\text{ dB}}(P_c)$, kHz	18	35	51
$f_{50\%}(P_c)$, kHz	31	57	95

The total charge and the capacitive components are computed as maximal amplitudes of P^* and P_c estimated at $\Psi_{DC}^e = -30$ mV.

components of the charge are taken into account. We find that for the same diffusion coefficient of 0.5×10^{-8} cm²/s, the capacitive component of the charge has the 3-dB and 50% frequencies equal to 18 and 31 kHz, while these frequencies for the total charge increase, respectively, to 31 and 54 kHz (Table 1). If both the resistive and capacitive components of charge movement are included in the analysis, the electrical frequency response can be closer to the flatter and broader mechanical responses of Frank and colleagues (Frank et al., 1999). This prediction requires further examination.

3.3. The phase shift and resistive component of transferred charge

We found a voltage-dependent phase shift between the transferred charge and the applied AC electric field (Fig. 3). The dependence of this angle on the DC component of the membrane potential is bell-shaped. Its minimum occurs at a potential where the voltage sensitivity of the transferred charge (P^*) is maximum (i.e., near -30 mV). For any DC potential, the phase shift is close to zero at low frequencies, and its absolute value monotonically increases with frequency approaching 90° for very high frequency (Fig. 4e). The phase shift is about 60° at frequency of 50 kHz and about 75° at 100 kHz. The phase shift is negative which means that the charge is delayed with respect to the membrane potential. The time derivative of this charge component is in phase with the applied AC field indicating an ohmic (resistive) electric current. This resistive component of charge transfer has been reported for a hydrophobic ion, dipicrylamine (DPA), movement through myocyte membrane (Lu et al., 1995) and for prestin-associated charge transfer in outer hair cells (Farrell et al., 2006).

The resistive part of the charge, P_r (Fig. 4c) is determined by $-\sin \theta$ (Fig. 3) and P^* (Fig. 4a), which increase and decrease with frequency, respectively. Their product increases with frequency up to a maximal value of about 0.5 at a frequency close to 40 kHz and then decreases when frequency further increases (see also Fig. 4d, presenting the resistive component of the charge as a function of frequency). While the resistive part of the transferred charge is not a monotonic function of frequency, its ratio to the capacitive is monotonic (Fig. 4e). This means that at low frequencies the transferred charge is of capacitive nature, but the resistive component becomes relatively more significant at higher frequencies. Thus, both components can be significant to high-frequency electromotility and active force production. The main predicted features of the transferred charge frequency dependence, such as a charge-electric field phase shift increasing with frequency, the monotonically decreasing capacitive component of the charge, and the charge resistive component having a single maximum, are similar (Fig. 4d) to the experimental observation of Lu and colleagues (Lu et al., 1995) of the hydrophobic ion of DPA movement across the myocyte membrane within a broad frequency range. Our analysis of the transferred charge components can stimulate further experiments to study high-frequency performance of prestin-containing cells.

3.4. Relation to other models of charge transfer by prestin

There have been a number of models proposed to explain the frequency (Iwasa, 1997; Dong et al., 2000) and voltage dependence of charge transfer by the membrane protein prestin (Oliver et al., 2001; Rybalchenko and Santos-Sacchi, 2003; Muallem and Ashmore, 2006). An early model (Iwasa, 1997; Dong et al., 2000) developed before the identification of prestin assumed that the outer hair cell motor (the charge) occupies two or three stable states where motor and charge transfer dynamics, including non-linear capacitance and current noise, were described by hypothe-

tical rate constants of switching from one state to the other. Experimental observations revealed a critical role for chloride ions binding to prestin (Oliver et al., 2001). In addition to chloride ions, the data presented in Oliver et al. (2001) demonstrate a role of internal protein charges in charge transfer, because their mutations cause shifts in voltage dependence of nonlinear capacitance. The role of chloride ions is the key part of recent models (Oliver et al., 2001; Rybalchenko and Santos-Sacchi, 2003). The first of the models relates the translocated charge with the chloride ion moving across a part of the membrane, and the second model suggests that charge movement is associated with a conformational change of prestin caused by the binding of chloride ions. More recently, a transport-based model (Muallem and Ashmore, 2006) was proposed to explain the reduction of charge transfer and shifts of the Q - Ψ function in the depolarization direction as a result of decreasing intracellular chloride ion concentration in outer hair cells (Fakler and Oliver, 2002). Charge transport in Muallem and Ashmore (2006) includes an ion of intracellular chloride binding the protein, its interaction with positive intrinsic protein charges, and exchange to a divalent ion of extracellular sulfate. These steps of transport are described in terms of several (eight) finite states of the protein and charge, including the corresponding rate constants. Three of pairs of the rate constants are voltage-dependent and others, not associated with the applied electric field, describe association/dissociation of ions (chloride and sulfate) to and from the protein. Presently, none of the models can explain all main data on electric charge transfer by prestin, in particular its frequency dependence. Here we propose a novel model that uses a Fokker–Planck equation to describe the kinetics of the translocated charge and give a physical basis for the frequency effect, including the cut-off frequency, where diffusion controls the magnitude of the charge and its phase shift relative to the applied electric field.

Prestin is critical to outer hair cell's role in high-frequency hearing (Lieberman et al., 2002; Dallos et al., 2008). Mammalian cells transfected with prestin show a constant frequency response to at least 20 kHz (Ludwig et al., 2001). Mammalian prestin is associated with the fastest molecular motor complex and active up to frequencies of several tens of kHz (Frank et al., 1999). The efficiency of the outer hair cell motor (Spector, 2005; Spector and Jean, 2004) is similar to other slower molecular motors such as myosin and kinesin that convert chemical into mechanical energy. Our model does not assume a finite number of states and hypothetical rate constants for charge switching between the states as used in previous analyses of prestin. Rather, in our consideration, the charge can occupy any position along its way across the protein, and this continuous path is characterized by a probability density function. In the present model, we have not included contributions from possible prestin conformational energy or the energy of the surrounding membrane. Additional energy terms will affect the quantitative details of the model, however, the overall modeling framework would be unchanged. The membrane composition could have a significant effect on prestin performance via redistribution of the local mechanical forces and (or) electric fields. Additional energetic contribution from the surrounding membrane is probably the next most important effect to include. These contributions will modify V in Eq. (1), and quantitative estimates of these effects are possible.

Our model can be used as a framework to compute the kinetic parameters of earlier finite state models as long as the detailed energy landscape of the protein is known (e.g., Xing et al., 2005). Phenomenological kinetic rate constants can be directly computed from the Fokker–Planck equation. Depending on the time regime of interest, the kinetic rate constant can have complex dependence on the applied oscillatory voltage. Our modeling provides a uniform explanation across different time regimes.

4. Conclusions

- (1) Prestin-associated charge movement is modeled with Fokker–Planck equation where we assume that a combination of chloride ions and intrinsic protein charges is translocated across the membrane.
- (2) Consistent with experiments, the model exhibits a voltage and frequency-dependent phase shift and resistive component of the transferred charge. The phase shift changes from zero at low frequencies toward -90° . The resistive component is bell-shaped in terms of voltage, and it has a single maximum as a function of frequency. The frequency affects the capacitive component in two ways, via the total amount of the transferred charge and the phase shift between the charge and the applied AC field.
- (3) By including both the capacitive and resistive components in the analysis of prestin-associated charge we show that the cut-off frequency can be extended, and it can help reconcile the discrepancy between the frequency responses of electrical and mechanical measurements.

Acknowledgments

This work was supported by NIH (NIDCD) research grants DC00354 and DC02775. We thank Shengran Feng for his help in FemLab simulations.

Appendix A. Supplementary material

Supplementary data associated with this article can be found in the online version at doi:10.1016/j.jtbi.2009.05.019.

References

- Ashmore, J.F., 1987. A fast motile response in guinea-pig outer hair cell: the cellular basis for cochlear amplifier. *J. Physiol.* 388, 323–347.
- Axelrod, D., Ravdin, P., Koppel, D.E., Schlessinger, J., Webb, W.W., Elson, E.L., Podleski, T.R., 1976. Lateral motion of fluorescently labeled acetylcholine receptors in membranes of developing muscle fibers. *Proc. Natl. Acad. Sci. USA* 73, 4594–4598.
- Benz, R., Nonner, W., 1981. Structure of the axolemma of frog myelinated nerve: relaxation experiments with a lipophilic probe ion. *J. Membr. Biol.* 59, 127–134.
- Brownell, W.E., Bader, C.R., Bertrand, D., Ribaupierre, Y., 1985. Evoked mechanical responses of isolated cochlear outer hair cell. *Science* 227, 194–196.
- Brownell, W.E., Spector, A.A., Raphael, R.M., Popel, A.S., 2001. Micro- and nanomechanics of the cochlear outer hair cell. *Annu. Rev. Biomed. Eng.* 3, 169–194.
- Dallos, P., Fakler, B., 2002. Prestin, a new type of motor protein. *Nat. Rev. Cell. Biol.* 3, 104–111.
- Dallos, P., Wu, X., Cheatham, M.A., Gao, J., Zheng, J., Anderson, C.T., Jia, S., Wang, X., Cheng, W.H.Y., Sengupta, S., He, D.Z., Zuo, J., 2008. Prestin-based outer hair cell motility is necessary for mammalian cochlear amplification. *Neuron* 58, 333–339.
- Deak, L., Zheng, J., Orem, A., Du, G.G., Aguinaga, S., Matsuda, K., Dallos, P., 2005. Effect of cyclic nucleotides on the function of prestin. *J. Physiol.* 563, 483–496.
- Dong, X.-X., Ehrenstein, D., Iwasa, K.H., 2000. Fluctuation of motor charge in the lateral membrane of the cochlear outer hair cell. *Biophys. J.* 79, 1876–1882.
- Fakler, B., Oliver, D., 2002. Functional properties of prestin—how the motor molecule works work. In: Gummer, A.W. (Ed.), *Biophysics of the Cochlea: From Molecules to Models*. World Scientific, New Jersey, pp. 110–115.
- Farrell, B., Ugrinov, R., Brownell, W.E., 2006. Frequency dependence of admittance and conductance of the outer hair cell. In: Nuttall, A.L., Ren, T., Gillespie, P., Grosh, K., de Boer, E. (Eds.), *Auditory Mechanisms. Processes and Models*. World Scientific, New Jersey, pp. 231–232.
- Fernandez, J.M., Taylor, R.E., Bezanilla, F., 1983. Induced capacitance in the squid giant axon. Lipophilic ion displacement currents. *J. Gen. Physiol.* 82, 331–346.
- Frank, G., Hemmert, W., Gummer, A.W., 1999. Limiting dynamics of high-frequency electromechanical transduction of outer hair cells. *Proc. Natl. Acad. Sci. USA* 96, 4420–4425.

- Gale, J., Ashmore, J.F., 1994. Charge displacement induced by rapid stretch in the basolateral membrane of the guinea-pig outer hair cell. *Proc. R. Soc. B* 255, 243–249.
- Gale, J., Ashmore, J.F., 1997a. An intrinsic frequency limit to the cochlear amplifier. *Nature* 389, 63–66.
- Gale, J.E., Ashmore, J.F., 1997b. The outer hair cell motor in membrane patches. *Pflugers Arch.* 434, 267–271.
- He, D.Z., Zheng, F., Kalinec, F., Kakehata, S., Santos-Sacchi, J., 2006. Tuning in to the amazing outer hair cell membrane wizardry with a twist and shout. *J. Membr. Biol.* 209, 119–134.
- Hille, B., 1984. *Channels of Excitable Membranes*. Sinauer Ass., Sunderland, Mass.
- Huang, G., Santos-Sacchi, J., 1994. Motility voltage sensor of the outer hair cell resides within the lateral plasma membrane. *Proc. Natl. Acad. Sci. USA* 91, 12268–12272.
- Iwasa, K.H., 1994. A membrane motor model for the fast motility of the outer hair cell. *J. Acoust. Soc. Am.* 96, 2216–2224.
- Iwasa, K.H., 1997. Current noise spectrum and capacitance due to the membrane motor of the outer hair cell: theory. *Biophys. J.* 73, 2965–2971.
- Jechiel, E., Edidin, M., 1987. Micrometer-scale domains in fibroblast plasma membrane. *J. Cell Biol.* 105, 755–760.
- Liao, Z., Feng, S., Popel, A.S., Brownell, W.E., Spector, A.A., 2007. Outer hair cell active force generation in the cochlear environment. *J. Acoust. Soc. Am.* 122, 2215–2225.
- Lieberman, M.C., Gao, J., He, D.Z., Wu, X., Jia, S., Zuo, J., 2002. Prestin is required for electromotility of the outer hair cell and for the cochlear amplifier. *Nature* 419, 300–304.
- Lu, C.-C., Kabakov, A., Markin, V.S., Mager, S., Frazer, G.A., Hilgemann, D.W., 1995. Membrane transport mechanisms probed by capacitance measurements with megahertz voltage clamp. *Proc. Natl. Acad. Sci. USA* 92, 11220–11224.
- Ludwig, J., Oliver, D., Frank, G., Kloker, N., Gummer, A.W., Fakler, B., 2001. Reciprocal electromechanical properties of rat prestin: the motor molecule from rat outer hair cells. *Proc. Natl. Acad. Sci. USA* 98, 4178–4183.
- de Monvel, J.B., Brownell, W.E., Ulfendahl, M., 2006. Lateral diffusion anisotropy and membrane lipid/skeleton interaction in outer hair cells. *Biophys. J.* 91, 364–381.
- Muallem, D., Ashmore, J.F., 2006. An anion antiporter model of prestin, the outer hair cell motor protein. *Biophys. J.* 90, 4035–4045.
- Navaratnam, D., Bai, J.-P., Samaranyake, H., Santos-Sacchi, J., 2005. N-terminal-mediated homogenization of prestin, the outer hair cell motor protein. *Biophys. J.* 89, 2252–3345.
- Oghalai, J.S., Zhao, H.B., Kutz, J.W., Brownell, W.E., 2000. Voltage- and tension-dependent lipid mobility in the outer hair cell plasma membrane. *Science* 287, 658–661.
- Oliver, D., He, D.Z., Kloker, N., Ludwig, J., Schulte, U., Waldegger, S., Rupperberg, J.P., Dallos, P., Fakler, B., 2001. *Science* 292, 2340–2343.
- Rajagopalan, L., Patel, N., Madabushi, S., Goddard, J.A., Aniat, V., Lin, F., Shope, S., Farrell, B., Lichtarge, O., Davidson, A., Brownell, W.E., Pereira, F.A., 2006. Essential helix interaction in the anion transporter domain revealed by evolutionary trace analysis. *J. Neurosci.* 26, 12727–12734.
- Rybalchenko, V., Santos-Sacchi, J., 2003. Cl⁻ flux through anion-selective, stretch-activated conductance influences the outer hair cell motor of the guinea-pig. *J. Physiol.* 547, 873–891.
- Santos-Sacchi, J., Digler, J.P., 1988. Whole cell currents and mechanical responses of isolated outer hair cells. *Hear. Res.* 35, 143–150.
- Santos-Sacchi, J., Kakehata, S., Kikuchi, T., Katori, Y., Takasaka, T., 1998. Density of motility-related charge in the outer hair cell of the guinea-pig is inversely related to best frequency. *Neurosci. Lett.* 256, 155–158.
- Schlaechinger, J.S., Oliver, D., 2007. Nonmammalian orthologs of prestin (SLC26A5) are electrogenic divalent/chloride anion transporters. *Proc. Natl. Acad. Sci. USA* 104, 7693–7698.
- Scherer, M.P., Gummer, A.W., 2004. How many states can the motor molecule, prestin, assume in an electric field. *Biophys. J.* 87, L27–L29.
- Spector, A.A., 2005. Active energy produced by molecular motors and nonlinear capacitance of cochlear outer hair cell. *J. Biomech. Eng.* 127, 391–399.
- Spector, A.A., Jean, R.P., 2004. Modes and balance of energy in the piezoelectric outer hair cell wall. *J. Biomech. Eng.* 126, 17–25.
- Spector, A.A., Deo, N., Grosh, K., Ratnanather, J.T., Raphael, R.M., 2006. Electromechanical models of the outer hair cell composite membrane. *J. Membr. Biol.* 209, 135–152.
- Xing, J., Wang, H., Oster, G., 2005. From continuum Fokker–Planck models to discrete kinetic models. *Biophys. J.* 89, 1551–1563.
- Zheng, J., Shen, W., He, D.Z., Long, K.B., Madison, L.D., Dallos, P., 2000. Prestin is the motor protein of cochlear outer hair cell. *Nature* 405, 149–155.
- Zheng, J., Long, K.B., Shen, W., Madison, L.D., Dallos, P., 2001. Prestin topology: localization of protein epitopes in relation to the plasma membrane. *NeuroReport* 12, 1929–1935.